

Copyright © 1992, by the author(s).
All rights reserved.

Permission to make digital or hard copies of all or part of this work for personal or classroom use is granted without fee provided that copies are not made or distributed for profit or commercial advantage and that copies bear this notice and the full citation on the first page. To copy otherwise, to republish, to post on servers or to redistribute to lists, requires prior specific permission.

BIFURCATION ANALYSIS OF CHUA'S CIRCUIT

by

Leon O. Chua and Luong T. Huynh

Memorandum No. UCB/ERL M92/96

15 July 1992

COVER PAGE

**BIFURCATION ANALYSIS OF CHUA'S
CIRCUIT**

by

Leon O. Chua and Luong T. Huynh

Memorandum No. UCB/ERL M92/96

15 July 1992

ELECTRONICS RESEARCH LABORATORY

College of Engineering
University of California, Berkeley
94720

This work is supported in part by the Office of Naval Research under grant N00014-89-J-1402 and the National Science Foundation under grant MIP-8912639.

**BIFURCATION ANALYSIS OF CHUA'S
CIRCUIT**

by

Leon O. Chua and Luong T. Huynh

Memorandum No. UCB/ERL M92/96

15 July 1992

ELECTRONICS RESEARCH LABORATORY

College of Engineering
University of California, Berkeley
94720

This work is supported in part by the Office of Naval Research under grant N00014-89-J-1402 and the National Science Foundation under grant MIP-8912639.

Bifurcation Analysis of Chua's Circuit

Leon O. Chua and Luong T. Huynh
University of California, Berkeley

Abstract—By transforming the state equation for Chua's circuit into a third order scalar differential equation, an explicit solution is obtained. This explicit solution can be used to make a computer program to calculate the trajectory of the circuit. The eigenvalues of the characteristic equation for each linear region can be categorized into different patterns. The diagrams of the eigenvalue patterns are found to belong to two groups. Within each group, the maps resemble each other qualitatively. Finally, the explicit solution is applied to trace period doublings up to a high period. The data are found to agree with the Feigenbaum number.

1 Introduction

In this paper, we will present results obtained on Chua's circuit by considering the exact solution of the differential vector equation representing the circuit. There has been a great number of literatures on this circuit and we will not attempt to repeat materials that are available elsewhere (see Chronological Bibliography). Rather, the three separate topics included in this paper are new materials and we find them worthwhile to be presented.

Chua's circuit (Figure 1) is a simple piecewise-linear third-order circuit. The state equation is given by

$$\begin{aligned} C_1 \frac{dv_{C_1}}{dt} &= G(v_{C_2} - v_{C_1}) - g(v_{C_1}) \\ C_2 \frac{dv_{C_2}}{dt} &= G(v_{C_1} - v_{C_2}) + i_L \\ L \frac{di_L}{dt} &= -v_{C_2} \end{aligned}$$

where $g(v_{C_1}) = G_b v_{C_1} + \frac{1}{2}(G_a - G_b)[|v_{C_1} + B_p| - |v_{C_1} - B_p|]$. By rescaling the variables, we can transform the state equation into a dimensionless form:

$$\frac{dx}{d\tau} = \alpha(y - x - f(x)) \quad (1)$$

$$\frac{dy}{d\tau} = x - y + z \quad (2)$$

$$\frac{dz}{d\tau} = -\beta y \quad (3)$$

where

$$f(x) = \begin{cases} m_1 x + m_0 - m_1, & x > 1 \\ m_0 x, & -1 \leq x \leq 1 \\ m_1 x - m_0 + m_1, & x < -1. \end{cases}$$

and

$$\begin{aligned} x &\equiv v_{C_1}/B_p, & y &\equiv v_{C_2}/B_p, & z &\equiv i_L/(B_p G), \\ \tau &\equiv tG/C_2, & m_0 &\equiv G_a/G, & m_1 &\equiv G_b/G, \\ \alpha &\equiv C_2/C_1, & \beta &\equiv C_2/(LG^2). \end{aligned}$$

For simplicity, we will be working in the dimensionless form and using t in place of τ . When $m_0 < -1$ and $-1 < m_1 < 0$, there are three equilibrium points of the form $(d, 0, -d)$.

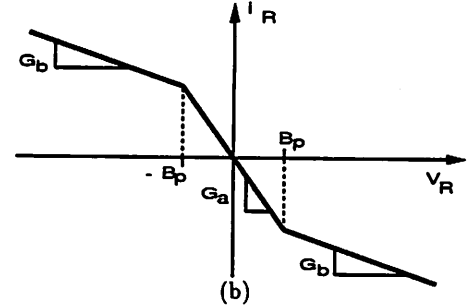
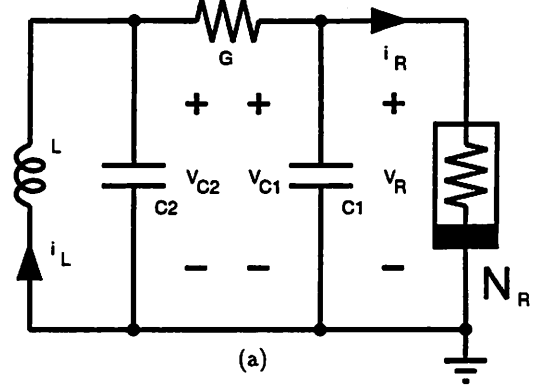


Figure 1: (a) Chua's circuit, and (b) v-i characteristic of the piecewise linear resistor.

$$d = \begin{cases} \frac{m_1 - m_0}{m_1 + 1}, & x > 1 \\ 0, & -1 \leq x \leq 1 \\ \frac{m_0 - m_1}{m_1 + 1}, & x < -1. \end{cases}$$

The above system of differential equation can be solved numerically using integration methods such as Runge-Kutta or Forward Euler. In Section 2, we will show that explicit solutions can be obtained which can be used to model the trajectory of the circuit with higher accuracy and speed. In Section 3, we will use the characteristic equation from Section 2 to investigate the eigenvalues patterns of the equation. In Section 4, we will show how the explicit equations make it possible to trace period doublings up to a high period and to verify the Feigenbaum number using data obtained.

2 Explicit Equations

In this section, we want to show that the Chua's circuit can be represented by a set of explicit equations. The derivation is based on the fact that within each linear region of the non-linear resistor, the differential equation representing Chua's circuit is linear. We begin by transforming the differential vector equation into a third-order scalar differential equation. From (3), we have

$$y = -\frac{1}{\beta}\dot{z} \quad (4)$$

$$\dot{y} = -\frac{1}{\beta}\ddot{z}. \quad (5)$$

From (2), (4), and (5),

$$\begin{aligned} -\frac{1}{\beta}\ddot{z} &= x + \frac{1}{\beta}\dot{z} + z \\ x &= -\left(\frac{1}{\beta}\ddot{z} + \frac{1}{\beta}\dot{z} + z\right) \end{aligned} \quad (6)$$

$$\dot{x} = -\left(\frac{1}{\beta}\dot{z}^{(3)} + \frac{1}{\beta}\ddot{z} + \dot{z}\right). \quad (7)$$

Substituting (4), (6) and (7) into (1) and simplifying, we obtain a third-order differential equation in z :

$$-\left(\frac{1}{\beta}\dot{z}^{(3)} + \frac{1}{\beta}\ddot{z} + \dot{z}\right) = -\frac{\alpha}{\beta}\dot{z} + \alpha(1+m)\left(\frac{1}{\beta}\ddot{z} + \frac{1}{\beta}\dot{z} + z\right) + \alpha(1+m)d$$

$$z^{(3)} + (1+\alpha+\alpha m)\ddot{z} + (\alpha m + \beta)\dot{z} + \alpha\beta(1+m)z + \alpha\beta(1+m)d = 0.$$

where m is equal to m_0 or m_1 , depending on which linear region is being considered. The characteristic equation is

$$s^3 + (1+\alpha+\alpha m)s^2 + (\alpha m + \beta)s + \alpha\beta(1+m) = 0.$$

and can be solved using Cardan's formulas. These formulas are available in mathematical handbooks and will not be given here. Let us call the three roots of this characteristic equation s_1 , s_2 , and s_3 . The solution for $z(t)$ is given by

$$z(t) = k_1 e^{s_1 t} + k_2 e^{s_2 t} + k_3 e^{s_3 t} - d.$$

From (4),

$$\begin{aligned} y(t) &= -\frac{1}{\beta}\dot{z} \\ &= -\frac{1}{\beta}k_1 s_1 e^{s_1 t} - \frac{1}{\beta}k_2 s_2 e^{s_2 t} - \frac{1}{\beta}k_3 s_3 e^{s_3 t}, \end{aligned}$$

and from (6),

$$\begin{aligned} x(t) &= \dot{y} + y - z \\ &= -\frac{1}{\beta}k_1(s_1^2 + s_1 + \beta)e^{s_1 t} - \frac{1}{\beta}k_2(s_2^2 + s_2 + \beta)e^{s_2 t} - \frac{1}{\beta}k_3(s_3^2 + s_3 + \beta)e^{s_3 t} + d. \end{aligned}$$

To solve for k_1 , k_2 , and k_3 , we first notice that the initial condition $(x(0), y(0), z(0))$ can be transformed into an equivalent initial condition in terms of z and its two derivatives at $t = 0$:

$$\begin{aligned} z(0) &= z(0) \\ \dot{z}(0) &= -\beta y(0) \\ \ddot{z}(0) &= -\beta \dot{y}(0) \\ &= -\beta[x(0) - y(0) + z(0)]. \end{aligned}$$

From the equation for $z(t)$,

$$\begin{aligned} z(0) &= k_1 + k_2 + k_3 - d \\ \dot{z}(0) &= k_1 s_1 + k_2 s_2 + k_3 s_3 \\ \ddot{z}(0) &= k_1 s_1^2 + k_2 s_2^2 + k_3 s_3^2. \end{aligned}$$

So that

$$\begin{aligned} \begin{bmatrix} k_1 \\ k_2 \\ k_3 \end{bmatrix} &= \begin{bmatrix} 1 & 1 & 1 \\ s_1 & s_2 & s_3 \\ s_1^2 & s_2^2 & s_3^2 \end{bmatrix}^{-1} \begin{bmatrix} z(0) + d \\ \dot{z}(0) \\ \ddot{z}(0) \end{bmatrix} \\ &= M \begin{bmatrix} z(0) + d \\ -\beta y(0) \\ -\beta[x(0) - y(0) + z(0)] \end{bmatrix}, \end{aligned}$$

where

$$M = \begin{bmatrix} \frac{s_2 s_3}{(s_1 - s_2)(s_1 - s_3)} & \frac{-(s_2 + s_3)}{(s_1 - s_2)(s_1 - s_3)} & \frac{1}{(s_1 - s_2)(s_1 - s_3)} \\ \frac{s_2 s_1}{(s_2 - s_3)(s_2 - s_1)} & \frac{-(s_2 + s_1)}{(s_2 - s_3)(s_2 - s_1)} & \frac{1}{(s_2 - s_3)(s_2 - s_1)} \\ \frac{s_1 s_2}{(s_3 - s_1)(s_3 - s_2)} & \frac{-(s_1 + s_2)}{(s_3 - s_1)(s_3 - s_2)} & \frac{1}{(s_3 - s_1)(s_3 - s_2)} \end{bmatrix}.$$

With these information available, it is possible to develop a computer program to find the trajectory of Chua's circuit using explicit equations. The program must keep track of the current linear region and use the appropriate eigenvalues for that region. Whenever the trajectory crosses a boundary of these regions (when $x = 1$ or $x = -1$), we use the values of x , y , and z at crossing, which can be obtained using the bisection or the Newton-Raphson method, as the initial condition for the next region.

3 Eigenvalue Patterns

In [8], it has been shown that two members of Chua's circuit family have the same qualitative behaviors if they have an identical set of eigenvalues in each linear region. It is useful therefore to obtain a relationship among α , β , and m such that the eigenvalues follow a certain pattern and to tabulate the possible patterns in the circuit. We will be interested in the signs and the relative magnitudes of the real components of the eigenvalues.

3.1 One Real and One Complex Conjugate Pair of Eigenvalues

Let us denote the eigenvalues by γ , $\sigma + j\omega$, and $\sigma - j\omega$. The characteristic equation is thus

$$s^3 + (-2\sigma - \gamma)s^2 + (\sigma^2 + 2\sigma\gamma + \omega^2)s + (-\sigma^2\gamma - \omega^2\gamma) = 0.$$

Equating the coefficients of the left hand side term by term with those of the characteristic equation, we have

$$\begin{aligned} 1 + \alpha + \alpha m &= -2\sigma - \gamma \\ \alpha m + \beta &= \sigma^2 + 2\sigma\gamma + \omega^2 \\ \alpha\beta(1 + m) &= -\sigma^2\gamma - \omega^2\gamma. \end{aligned}$$

We are interested in the values of the parameters such that $\sigma = 0$, $\gamma = 0$, $\gamma = \sigma$, and $\omega = 0$. These can be obtained through algebraic manipulations on the above equations and are given below. Since these equations only work when there is a pair of complex conjugate eigenvalues, we disregard the segments of these curves that lie inside the all real eigenvalues regions. The boundary of the real eigenvalues regions is the curve $\omega = 0$.

$$\begin{aligned} \sigma = 0: & \quad \beta = -\alpha m(1 + \alpha + \alpha m) \\ \gamma = 0: & \quad \alpha = 0 \text{ or } \beta = 0 \end{aligned}$$

$$\begin{aligned}
\gamma = \sigma: \quad \beta &= \frac{(1 + \alpha + am)(am - \frac{2}{9}(1 + \alpha + am)^2)}{2\alpha + 2am - 1} \\
\gamma = -\sigma: \quad \beta &= -\frac{(1 + \alpha + am)(am + 2(1 + \alpha + am)^2)}{2\alpha + 2am + 1} \\
\omega = 0: \quad \begin{cases} \alpha = -\frac{\sigma - 2\sigma^2 + \sigma\sqrt{(1+2\sigma)/(1+m)}}{2\sigma + 2\sigma m + m} \\ \beta = -\sigma - \sigma^2 - \sigma\sqrt{(1+2\sigma)/(1+m)} \end{cases} \text{ or } \\
\begin{cases} \alpha = -\frac{\sigma - 2\sigma^2 - \sigma\sqrt{(1+2\sigma)/(1+m)}}{2\sigma + 2\sigma m + m} \\ \beta = -\sigma - \sigma^2 + \sigma\sqrt{(1+2\sigma)/(1+m)} \end{cases}
\end{aligned}$$

3.2 Three Real Eigenvalues

The equation for three real eigenvalues is given by

$$s^3 + (-\gamma_1 - \gamma_2 - \gamma_3)s^2 + (\gamma_1\gamma_2 + \gamma_2\gamma_3 + \gamma_3\gamma_1)s + (-\gamma_1\gamma_2\gamma_3) = 0$$

where γ_1, γ_2 , and γ_3 are the roots, such that $\gamma_1 < \gamma_2 < \gamma_3$. Comparing the last term on the left hand side with that of the characteristic equation, we see that the condition for one eigenvalue to be zero is $\alpha = 0$ or $\beta = 0$.

3.3 Eigenvalue Pattern Diagrams

The equations given in Subsections 3.1 and 3.2 have been plotted on the α, β plane for $m_0 = -8/7$ and $m_1 = -5/7$ in Figure 2. These curves describe the boundaries of regions with the same eigenvalue pattern. In these diagrams, the patterns are coded as following:

| | | |
|-------------|--|---|
| RCO | $\Leftrightarrow \gamma < \sigma < 0$ | $\begin{array}{c} \times \\ \times \end{array} \text{---}$ |
| CRO | $\Leftrightarrow \sigma < \gamma < 0$ | $\begin{array}{c} \times \\ \times \end{array} \text{---}$ |
| $\bar{C}OR$ | $\Leftrightarrow \sigma < 0 < \gamma, \sigma > \gamma $ | $\begin{array}{c} \times \\ \times \end{array} \text{---} \times$ |
| COR | $\Leftrightarrow \sigma < 0 < \gamma, \sigma < \gamma $ | $\begin{array}{c} \times \\ \times \end{array} \text{---} \times$ |
| OCR | $\Leftrightarrow 0 < \sigma < \gamma$ | $\text{---} \begin{array}{c} \times \\ \times \end{array} \times$ |
| ORC | $\Leftrightarrow 0 < \gamma < \sigma$ | $\text{---} \times \begin{array}{c} \times \\ \times \end{array}$ |
| $RO\bar{C}$ | $\Leftrightarrow \gamma < 0 < \sigma, \sigma > \gamma $ | $\text{---} \times \begin{array}{c} \times \\ \times \end{array}$ |
| $\bar{R}OC$ | $\Leftrightarrow \gamma < 0 < \sigma, \sigma < \gamma $ | $\times \begin{array}{c} \times \\ \times \end{array}$ |
| $RRRO$ | $\Leftrightarrow \gamma_1 < \gamma_2 < \gamma_3 < 0$ | $\times \times \times \text{---}$ |
| $RROR$ | $\Leftrightarrow \gamma_1 < \gamma_2 < 0 < \gamma_3$ | $\times \times \text{---} \times$ |
| $RORR$ | $\Leftrightarrow \gamma_1 < 0 < \gamma_2 < \gamma_3$ | $\times \text{---} \times \times$ |
| $ORRR$ | $\Leftrightarrow 0 < \gamma_1 < \gamma_2 < \gamma_3$ | $\text{---} \times \times \times$ |

The mnemonics is as follow: R stands for a real eigenvalue, C stands for the real part of the complex conjugate eigenvalues, and O stands for 0. The letters are arranged in increasing order and a bar on top is used to denote the one with larger magnitude when R and C are on opposite sides of O . In the O region, m_0 is used for m and in P^\pm region, m_1 is used. The pattern combination will be written in the form

(code for O , code for P^\pm).

It is found that the diagram for $m_0 = -8/7$ also gives a qualitative picture for all $m_0 < -1$. In other words, all diagrams for $m_0 < -1$ resemble that of $m_0 = -8/7$ in connections and positions of curves. Similarly, the diagram for $m_1 = -5/7$ also gives a qualitative picture for all $-1 < m_1 < 0$. As a result, the diagrams can be divided into two groups: $m_0 < -1$ in O region and $-1 < m_1 < 1$ in P^\pm region.

By varying m_0 from $-\infty$ to -1 and m_1 from -1 to 0 , we have tabulated the possible combinations of eigenvalues for the circuit. They are given in Table 1.

We would like to note that since the curve for $\sigma = 0$ does not exist for $m_0 < -1$, there is no Hopf at O . Looking at the diagrams, we see that Hopf at P^\pm occurs when the eigenvalue combination varies from (COR, RCO) into $(COR, \bar{R}OC)$ in the first quadrant. The parameters for Hopf can be calculated exactly using the equation for $\sigma = 0$ in P^\pm region. In the third quadrant (α and β are both negative), there is another path for Hopf at P^\pm across the boundary between $(\bar{C}OR, RCO)$ and $(\bar{C}OR, \bar{R}OC)$, but this region has not been fully investigated due to time constraint of this writing. In Chua's Circuit, period bifurcations and chaotic attractors have been found in the $(COR, \bar{R}OC)$ region.

4 Period Doublings

We will fix β at 16, m_0 at $-8/7$, and m_1 at $-5/7$, and calculate the α 's at which period doublings occur. These α 's are then used to verify the Feigenbaum number.

Our method includes finding a periodic trajectory for a given set of parameters α, β, m_0 , and m_1 and testing for the stability of the trajectory. Suppose a trajectory $\Phi^t(x_0, y_0, z_0)$ originating from $\Phi^0 = (x_0, y_0, z_0)$ has period T , then just before it loses stability to double in period, two of the three eigenvalues of the Jacobian $(D\Phi^T)_{(x_0, y_0, z_0)}$ has magnitude unity (two characteristic exponents are zero and the third one is negative). One magnitude unity eigenvalue is due to the fact that the trajectory is periodic. The second one is due to the fact that the trajectory is almost a saddle-type periodic orbit.

The periodic trajectory was obtained by solving for an equilibrium point Φ^0 such that $\Phi^T(\Phi^0) = \Phi^0$. This was not trivial and involved much trial and error work. As a result, we will not give details on this.

The Jacobian matrix $(D\Phi^T)_{\Phi^0}$ of the periodic orbit is obtained using the following method. From the equations for $x(t), y(t)$, and $z(t)$ in Section 2, we see that the trajectory Φ^t depends linearly on k_1, k_2 , and k_3 which in turn depend linearly on Φ^0 , the initial condition of the current linear region. Therefore, $(D\Phi^t)_{\Phi^0}$ is independent of the initial condition. Knowing the time t a trajectory spends continuously in a linear region enables us to calculate the Jacobian for the segment of the trajectory that lies in the region. The columns of the matrix are given by $\Phi^t(1, 0, 0)$, $\Phi^t(0, 1, 0)$, and $\Phi^t(0, 0, 1)$. To calculate the

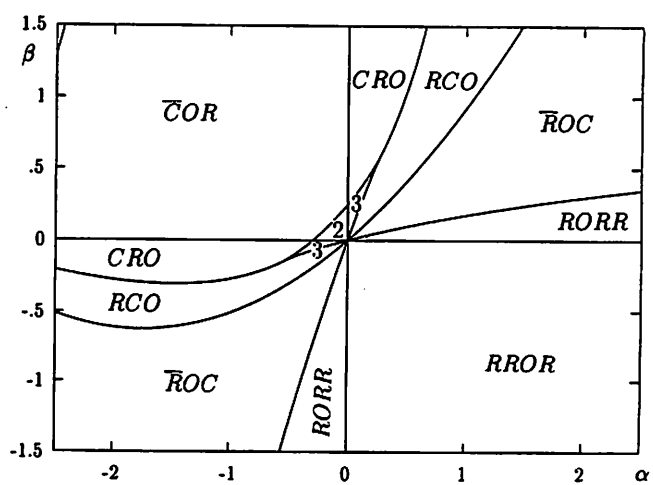
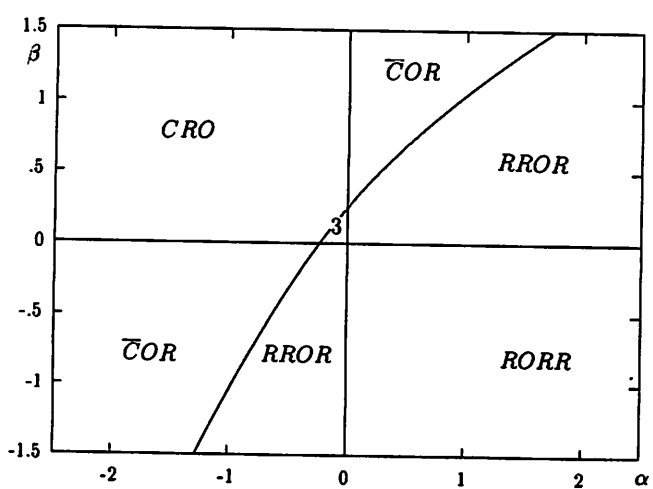
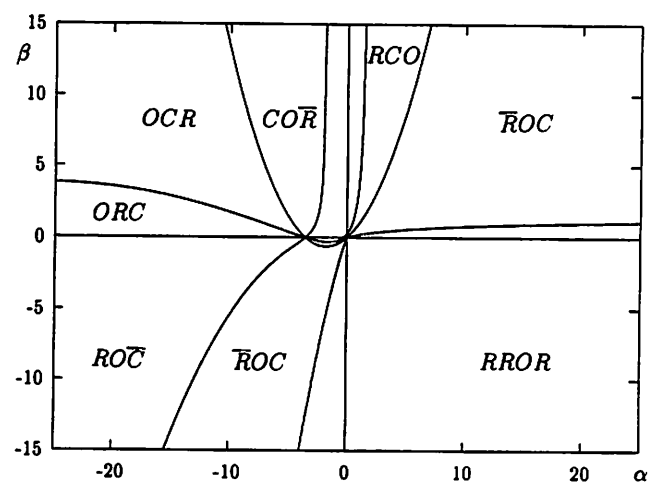
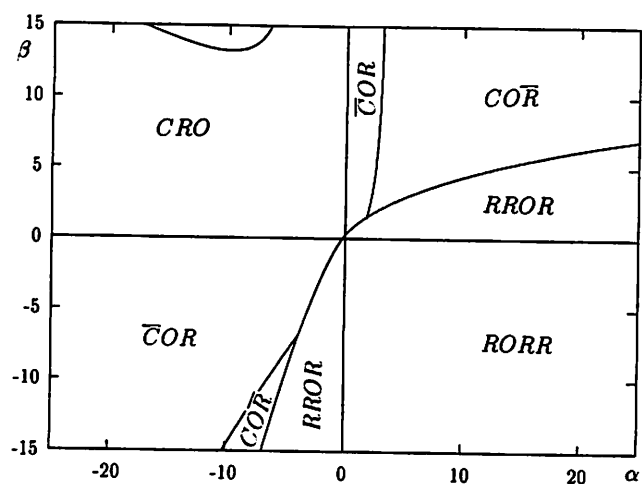
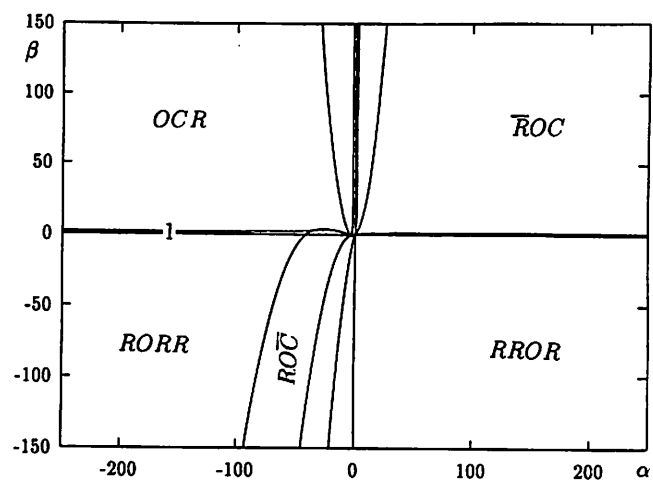
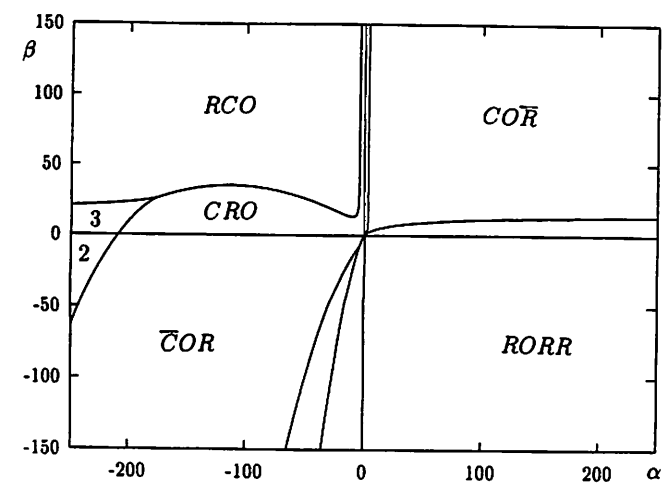


Figure 2: Eigenvalue patterns diagrams. Left column: $m_0 < -1$ (O region). Right column: $-1 < m_1 < 1$ (P^\pm region). 1: $ORRR$, 2: $RROR$, 3: $RRRO$.

| O Region | P [±] Region | | | | | | | | | | | |
|-------------|-----------------------|-------------------|-------|-------|-------|-------|------------------|------------------|--------|--------|--------|--------|
| | $\overline{C}OR$ | $COR\overline{R}$ | OCR | ORC | CRO | RCO | $\overline{R}OC$ | $RO\overline{C}$ | $RRRO$ | $RROR$ | $RORR$ | $ORRR$ |
| COR | | | | | Y | Y | Y | Y | Y | | Y | |
| COR | | | | | Y | Y | Y | Y | Y | | Y | |
| OCR | | | | | | | | | | | | |
| ORC | | | | | | | | | | | | |
| CRO | Y | Y | Y | Y | | | | | | Y | | Y |
| RCO | Y | Y | Y | Y | | | | | | | | Y |
| ROC | | | | | | | | | | | | |
| ROC | | | | | | | | | | | | |
| $RRRO$ | Y | Y | Y | Y | | | | | | Y | | Y |
| $RROR$ | | | | | Y | Y | Y | Y | Y | | Y | |
| $RORR$ | | | | | | | | | | Y | | |
| $ORRR$ | | | | | | | | | | | | |

Table 1: Possible eigenvalues patterns combinations. Y: yes, blank: no.

overall Jacobian. we start with a 3×3 unit matrix and premultiply by the Jacobian for each region until the trajectory has completed its period. The overall Jacobian can then be used to solve for the eigenvalues.

The α 's at which a periodic trajectory loses stability are listed in Table 2. The ratios of successive $\Delta\alpha$'s agree with the Feigenbaum number almost up to five digits at period 256. The bifurcation diagram in Figure 3 shows the bifurcation evolution as α increases.

| Onset of Period | α at Onset | Ratio of Difference |
|-----------------|-------------------|---------------------|
| 2 | 8.855726163 | |
| 4 | 9.1080893023 | |
| 8 | 9.1591511652 | 4.94230 |
| 16 | 9.16997924215 | 4.71569 |
| 32 | 9.17229337816 | 4.67910 |
| 64 | 9.17278877717 | 4.67126 |
| 128 | 9.172894866343 | 4.66965 |
| 256 | 9.172917586935 | 4.66930 |

Table 2: Period doublings for $\beta = 16$, $m_0 = -8/7$, and $m_1 = -5/7$. The value in the last column is calculated using the last three α 's. For example, the first value is equal to $(\alpha_4 - \alpha_2)/(\alpha_8 - \alpha_4)$.

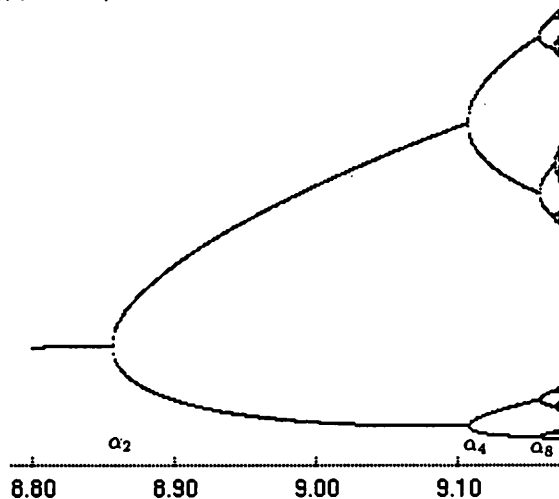


Figure 3: Period doublings as α is increased from period 1.

Chronological Bibliography

- [1] T. Matsumoto, "A chaotic attractor from Chua's circuit," *IEEE Trans. Circuits Syst.*, vol. CAS-31, no. 12, pp. 1055–1058, 1984.
- [2] G. Q. Zhong and F. Ayrom, "Experimental confirmation of chaos from Chua's circuit," *Int. J. Circuit Theory Appl.*, vol. 13, no. 11, pp. 93–98, 1985.
- [3] T. Matsumoto, L. O. Chua, and M. Komuro, "The Double Scroll," *IEEE Trans. Circuits Syst.*, vol. CAS-32, no. 8, pp. 797–818, 1985.
- [4] G. Q. Zhong and F. Ayrom, "Periodicity and chaos in Chua's circuit," *IEEE Trans. Circuits Syst.*, vol. CAS-32, no. 5, pp. 501–503, 1985.
- [5] F. Ayrom and G. Q. Zhong, "Chaos in Chua's circuit," *Proc. IEE*, vol. 133, pp. 307–312, November 1986.
- [6] T. Matsumoto, L. O. Chua, and K. Tokumasu, "Double Scroll via a two-transistor circuit," *IEEE Trans. Circuits Syst.*, vol. CAS-33, no. 8, pp. 828–835, 1986.
- [7] T. Matsumoto, L. O. Chua, and M. Komuro, "The Double Scroll bifurcations," *Int. J. Circuit Theory Appl.*, vol. 14, no. 1, pp. 117–146, 1986.
- [8] L. O. Chua, M. Komuro, and T. Matsumoto, "The Double Scroll family, parts I and II," *IEEE Trans. Circuits Syst.*, vol. CAS-33, no. 11, pp. 1073–1118, 1986.
- [9] T. S. Parker and L. O. Chua, "The dual Double Scroll equation," *IEEE Trans. Circuits Syst.*, vol. CAS-34, no. 9, pp. 1059–1073, 1987.
- [10] M. E. Broucke, "One-parameter bifurcation diagram for Chua's circuit," *IEEE Trans. Circuits Syst.*, vol. CAS-34, no. 3, pp. 208–209, 1987.
- [11] L. Yang and Y. L. Liao, "Self-similar structures from Chua's circuit," *Int. J. Circuit Theory Appl.*, vol. 15, pp. 189–192, 1987.
- [12] T. Matsumoto, L. O. Chua, and R. Tokunaga, "Chaos via torus breakdown," *IEEE Trans. Circuits Syst.*, vol. CAS-34, no. 3, pp. 240–253, 1987.
- [13] T. Matsumoto, L. O. Chua, and M. Komuro, "Birth and death of the Double Scroll," *Physica*, vol. 24D, pp. 97–124, 1987.
- [14] M. J. Ogorzalek, "Chaotic regions from Double Scroll," *IEEE Trans. Circuits Syst.*, vol. CAS-34, no. 2, pp. 201–203, 1987.
- [15] S. Wu, "Chua's circuit family," *Proc. IEEE*, vol. 75, no. 8, pp. 1022–1032, 1987.
- [16] A. I. Mees and P. B. Chapman, "Homoclinic and heteroclinic orbits in the Double Scroll attractor," *IEEE Trans. Circuits Syst.*, vol. CAS-34, no. 9, pp. 1115–1120, 1987.
- [17] C. Kahlert and L. O. Chua, "Transfer maps and return maps for piecewise-linear and three-region dynamical systems," *Int. J. Circuit Theory Appl.*, vol. 15, pp. 23–49, 1987.

- [18] C. Kahlert, "The range of transfer and return maps in three-region piecewise-linear dynamical systems," *Int. J. Circuit Theory Appl.*, vol. 16, pp. 11–23, 1988.
- [19] C. Kahlert, "Dynamics of the inclusions appearing in the return maps of Chua's circuit - 1. the creation mechanism," *Int. J. Circuit Theory Appl.*, vol. 17, no. 1, pp. 29–46, 1988.
- [20] C. Kahlert, "The chaos producing mechanism in Chua's circuit," *Int. J. Circuit Theory Appl.*, vol. 16, no. 4, pp. 227–232, 1988.
- [21] C. P. Silva and L. O. Chua, "The overdamped Double Scroll family," *Int. J. Circuit Theory Appl.*, vol. 16, no. 7, pp. 223–302, 1988.
- [22] T. Matsumoto, L. O. Chua, and K. Ayaki, "Reality of chaos in the Double Scroll circuit: A computer-assisted proof," *IEEE Trans. Circuits Syst.*, vol. CAS-35, no. 7, pp. 909–925, 1988.
- [23] P. Bartissol and L. O. Chua, "The Double Hook," *IEEE Trans. Circuits Syst.*, vol. CAS-35, no. 12, pp. 1512–1522, 1988.
- [24] M. Komuro, "Normal forms of continuous piecewise-linear vector fields and chaotic attractors: Part I," *Japan J. Appl. Math.*, vol. 5, no. 2, pp. 257–304, 1988.
- [25] M. Komuro, "Normal forms of continuous piecewise-linear vector fields and chaotic attractors: Part II," *Japan J. Appl. Math.*, vol. 5, no. 3, pp. 503–549, 1988.
- [26] R. Tokunaga, T. Matsumoto, M. Komuro, L. O. Chua, and K. Miya, "Homoclinic linkage: A new bifurcation mechanism," *Proc. IEEE ISCAS*, vol. 2, pp. 826–829, 1989.
- [27] R. Tokunaga, T. Matsumoto, T. Ida, and K. Miya, "Homoclinic linkage in the Double Scroll circuit and the cusp-constrained circuit," in *The Study of Dynamical Systems* (N. Aoki, ed.), pp. 192–209, Singapore: World Scientific, 1989.
- [28] M. Komuro, "Bifurcation equations of 3-dimensional piecewise-linear vector fields," in *Bifurcation Phenomena in Nonlinear Systems and Theory of Dynamical Systems* (H. Kawakami, ed.), pp. 113–123, Singapore: World Scientific, 1990.
- [29] C. M. Blazquez and E. Tuma, "Dynamics of the Double Scroll circuit," *IEEE Trans. Circuits Syst.*, vol. CAS-37, no. 5, pp. 589–593, 1990.
- [30] L. O. Chua and G. N. Lin, "Canonical realization of Chua's circuit family," *IEEE Trans. Circuits Syst.*, vol. CAS-37, no. 7, pp. 885–902, 1990.
- [31] L. O. Chua and G. N. Lin, "Intermittency in a piecewise-linear circuit," *IEEE Trans. Circuits Syst.*, vol. CAS-38, no. 5, pp. 510–520, 1990.
- [32] R. Lozi and S. Ushiki, "Confinors and bounded-time patterns in Chua's circuit and the Double Scroll family," *Int. J. Bifurcation and Chaos*, vol. 1, no. 1, pp. 119–138, 1991.
- [33] R. Lozi and S. Ushiki, "Coexisting chaotic attractors in Chua's circuit," *Int. J. Bifurcation and Chaos*, vol. 1, no. 4, pp. 923–926, 1991.
- [34] M. Komuro, R. Tokunaga, T. Matsumoto, and A. Hotta, "Global bifurcation analysis of the Double Scroll circuit," *Int. J. Bifurcation and Chaos*, vol. 1, no. 1, pp. 139–182, 1991.
- [35] C. Kahlert, "Heteroclinic orbits and scaled similar structures in the parameter space of the Chua oscillator," in *Chaotic Hierarchy* (G. Baier and M. Klein, eds.), pp. 209–234, Singapore: World Scientific, 1991.
- [36] J. M. Cruz and L. O. Chua, "A CMOS IC nonlinear resistor for Chua's circuit," ERL memorandum, Electronics Research Laboratory, University of California at Berkeley, CA 94720, 20 February 1992.
- [37] V. Perez-Munuzuri, V. Perez-Villar, and L. Chua, "Traveling wave front and its failure in a one-dimensional array of Chua's circuits," ERL memorandum, Electronics Research Laboratory, University of California at Berkeley, CA 94720, 22 April 1992.
- [38] V. Anishchenko, M. Safonova, and L. Chua, "Stochastic resonance in Chua's circuit," *International Journal of Bifurcation and Chaos*, vol. 2, no. 2, pp. 397–401, 1992.
- [39] V. Perez-Munuzuri, V. Perez-Villar, and L. Chua, "Propagation failure in linear arrays of Chua's circuit," *International Journal of Bifurcation and Chaos*, vol. 2, no. 2, pp. 403–406, 1992.